JOURNAL OF MATERIALS SCIENCE 10 (1975) 406–414

Relationship between atomic ordering and fracture in Fe–Al alloys

M. J. MARCINKOWSKI, M. E. TAYLOR
Engineering Materials Group, and Department of Mechanical Engineering, University of Maryland, College Park, Maryland, USA

F. X. KAYSER
Ames Laboratory USAEC, and Department of Metallurgy, Iowa State University, Ames, Iowa, USA

The fracture surfaces of slowly cooled Fe–Al alloys containing up to 28 at. % Al were examined using scanning electron microscopy techniques. It was found that the fracture modes changed from void coalescence to transgranular and finally, to intergranular as the Al concentration increased. The latter two modes of fracture were of the brittle type and were associated with the onset of long range order in these alloys. In particular, it has been postulated that atomic ordering leads to markedly reduced cross-slip, in turn reducing the degree to which void coalescence, with accompanying ductility, can occur.

1. Introduction

It has been known for some time that atomic ordering leads to pronounced brittle fracture in many alloys. In particular, such embrittlement has been observed in FeCo [1, 2], Ni_3Mn [3], FeAl [1], FeCo–2V [4-9], Fe_3Al [10-12], Fe_3Si [13], β-brass [14-16], NiAl [17, 18] and Ni_3Al [17] superlattices. Whereas the type of fracture in FeCo–2V [7, 19] and β-brass [14, 15] has been reported to be of either the transgranular or intergranular type, depending upon temperature, the fractures in FeCo [1, 2], Fe_3Al [10-12], NiAl [17, 18] and FeAl [1] have been observed to be of the intergranular type. Similarly, in fatigued samples of Ni_3Mn [20], FeCo–2V [20] and β-brass [21], the cracks were observed to be of the intergranular type. A number of hypotheses have been proposed to account for the brittle behaviour of ordered alloys. On the one hand, it has been argued that the embrittlement results from the build up of high internal stress concentrations due to the difficulty of cross-slip in ordered alloys [19]. On the other hand, it has been postulated that impurity segregation at the grain boundaries might be responsible for the brittle intergranular fracture that is observed [22, 23]. A third possibility has also been advanced, which is related to the inherent structure of a grain boundary in an ordered alloy [24-27]. This can be most readily seen by reference to Fig. 1 which shows an 18.9° symmetrical tilt boundary in a simple ordered lattice. It is apparent that the grain boundary is comprised of a vertical array of edge dislocations, and that each alternate pair of such dislocations has associated with it wrong or like nearest neighbour atom pairs across the grain boundary. In the limit of low-angle boundaries, the boundary may be visualized as an array of vertically aligned superlattice dislocations, i.e. a pair of ordinary dislocations connected by an antiphase boundary [28, 29]. It follows, therefore, that both high-angle and low-angle grain boundaries in ordered alloys possess higher energies relative to the grain interior, as compared to the corresponding disordered alloys, due to the disorder within the grain boundary. The grain boundaries thus provide a relatively high energy path for the nucleation and/or propagation of cracks, compared to that of the ordered grain interior.

So far, no systematic study has been carried out of the fracture morphology of superlattice alloys over a range of compositions extending from one of the pure components to the stoichiometric fully ordered alloy. Since many pure metals exhibit relatively ductile fractures, such a study would provide a means of observing, in a

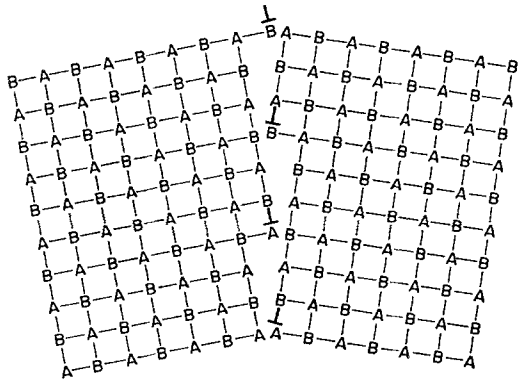

Figure 1 An 18.9° symmetric tilt boundary in a simple ordered lattice.

systematic manner, the transition from ductile to brittle fracture brought about by atomic ordering. It was therefore decided to examine the tensile fracture surfaces of Fe–Al alloys extending from nearly pure iron to approximately the stoichiometric Fe_3Al composition. The method of observation selected was that of scanning electron microscopy. This choice was dictated by the combination of high depth of field and high resolution (approximately 150 Å) attainable with the scanning electron microscope (SEM).

2. Experimental procedures

The samples used in the present study were obtained from fractured tensile specimens which were part of an earlier investigation concerning the mechanical properties of Fe–Al alloys [11, 30, 31]. The samples contained from 80 to 120 ppm carbon and from 30 to 90 ppm nitrogen [10], while the aluminium contents ranged from 1.0 to 30.7 at. % and were certain to within $\pm$ 0.1 at. % Al. All samples were slowly cooled to various temperatures in order to maintain the equilibrium values of atomic order characteristic of that temperature and pulled to fracture at this temperature. The test temperatures employed were 298, 477, 589, 708, 809 and 839 K. Samples tested at 589 K and above were sufficiently well oxidized to raise questions concerning the nature of the true fracture surface, and were therefore not examined. Approximately $\frac{1}{4}$ in. lengths were cut from one of the fractured ends of several of the $\frac{1}{4}$ in. diameter tensile specimens. These pieces were, in turn, mounted on pedestals with conducting cement and examined within the Cambridge "Stereoscan" SEM operating at 20 kV.

3. Experimental results and discussion

Because of the qualitative similarity in mechanical properties [12] between the samples tested at 298 and 477 K, as well as the greater number of compositions available corresponding to the 477 K specimens, it was decided to examine only those fracture surfaces associated with the 477 K tests. Fig. 2 shows the per cent reduction in areas as a function of aluminium concentration for alloys slowly cooled to 477 K and tested in tension to fracture at this same temperature.

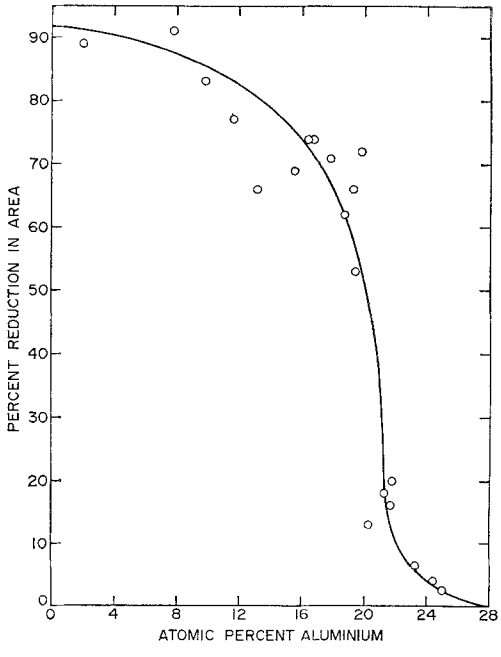

Figure 2 Ductility of iron–aluminium alloys that were slowly cooled to 477 K and fractured in tension at this temperature.

Fig. 3a shows a scanning electron micrograph of the fracture surface obtained from a 2 at. % Al sample where the electron beam was oriented nearly perpendicular to the fracture surface. The fracture surface is seen to consist of a very large number of coalesced voids or cavities which are quite characteristic of ductile materials [32]. Examination of Fig. 2 shows that this particular sample has undergone an 89 % reduction in area. Fig. 3b is a scanning electron micrograph from the same sample as that from which Fig. 3a was obtained, but from a different area and with the beam oriented 40° with respect to the fracture surface. The voids now take on a characteristic parabolic appearance, because of the tilt of the

beam with respect to the fracture surface. The schematic illustrations in Fig. 4a and b show more clearly the process of void formation and coalescence under an applied tensile stress, σ, which leads to ductile fracture. The nucleation of these voids has been associated with various types of defects within the crystal [29, 32-34].

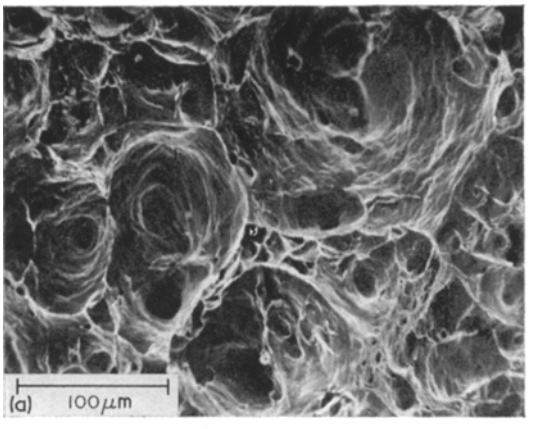

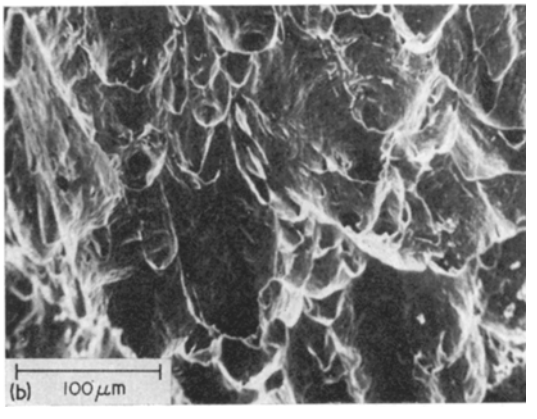

Figure 3 (a) Scanning electron micrograph of the fracture surface of a fully ductile 2 at. % Al alloy illustrating fracture by void coalescence. Electron beam was oriented normal to the fracture surface. (b) Scanning electron micrograph from the same sample as that described in (a) but from a different area, and with the electron beam oriented 40° with respect to the fracture surface.

Fig. 5a and b show scanning electron micrographs of the fracture surfaces characteristic of alloys containing 7.8% and 16.4 at. % Al, respectively. Along with the decrease in ductility accompanying this increased Al concentration, as can be seen from Fig. 2, the scanning electron micrographs in Fig. 5a and b show a corresponding decrease in void size when compared to the lower Al content alloy represented in Fig. 3. With still higher Al contents, i.e. 18.8 at. %, Fig. 6 shows the development of more well-defined planar fracture surfaces, in addition to the voids observed in the earlier samples. This situation is illustrated schematically in Fig. 7. In particular, these observations show that fracture in the 18.8 at. % Al alloy does not occur by void coalescence, but by isolated void formation and subsequent transgranular cleavage through the voids. As the Al concentration is increased still further to 21.8 at. %, transgranular cleavage begins to become the predominant mode of fracture, as can be seen by the scanning electron micrograph of Fig. 8a. That some void formation is still taking place is evidenced by the scanning electron micrograph of Fig. 8b. However, the size and extent of these voids is drastically reduced compared to the more ductile alloys. In addition, Fig. 2 shows that the ductility has also been reduced to about 20%. Close examination of Fig. 8 shows that some intergranular fracture is beginning to occur, however, the predominant fracture mode is transgranular, characterized by numerous river line patterns. These river lines are undoubtedly

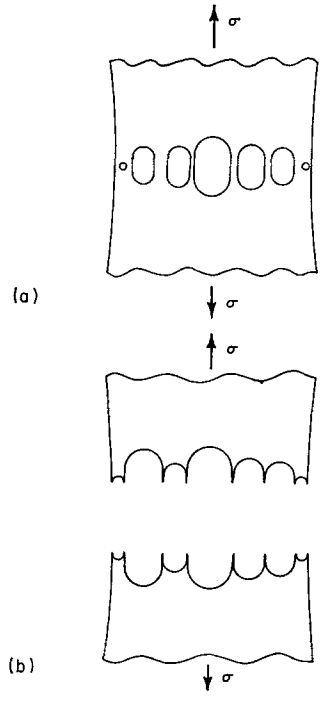

Figure 4 (a) Void formation in a ductile alloy. (b) Fracture by void coalescence in the same alloy.

generated by the intersection of the crack with pre-existing defects such as grain boundaries (both high- and low-angle types) and dislocations [32, 34, 35].

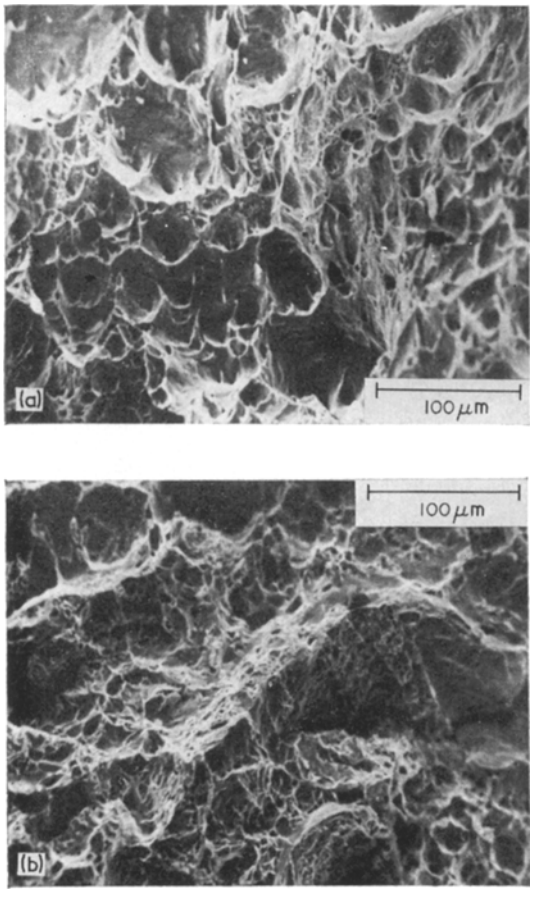

Figure 5 (a) Scanning electron micrograph of the fracture surface in a ductile 7.8 at. % Al alloy. Electron beam was oriented 45° with respect to the fracture surface. (b) Scanning electron micrograph of the fracture surface in a ductile 16.4 at. % Al alloy. Electron beam was oriented nearly normal to the fracture surface.

Fig. 9a shows that at an Al concentration of 25.5 at. %, the fracture becomes predominantly intergranular with some vestiges of transgranular cleavage still remaining. This is in keeping with previous results obtained for a 50 at. % Al alloy which fractured entirely by means of the intergranular mode [1]. A somewhat higher magnification of the central area of Fig. 9a is shown in Fig. 9b. The smooth nature of the fracture surface [1, 32], a characteristic of intergranular fracture,

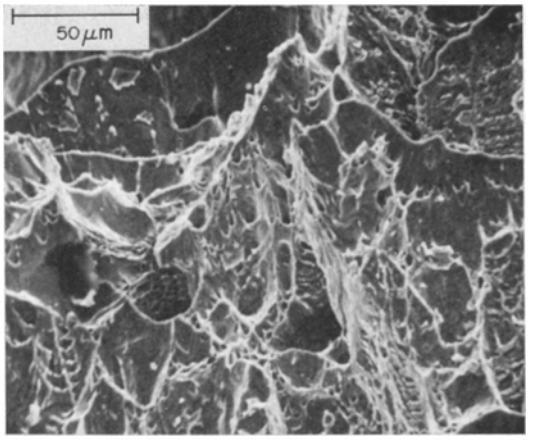

Figure 6 Scanning electron micrograph of the fracture surface in a partially embrittled 18.8 at. % Al alloy. Electron beam was oriented 52° with respect to the fracture surface.

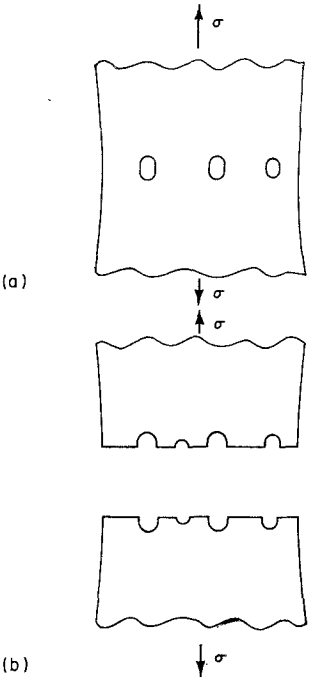

Figure 7 (a) Void formation in a partially embrittled alloy. (b) Fracture by cleavage in the same alloy.

is immediately apparent in this figure. Several grain-boundary inclusions can also be seen attached to the surfaces of the grains, which were previously grain boundaries. Reference to Fig. 2 also shows that the ductility of the 25.5 at. % Al alloy has essentially been reduced to zero.

Comparison of the results shown in Fig. 2

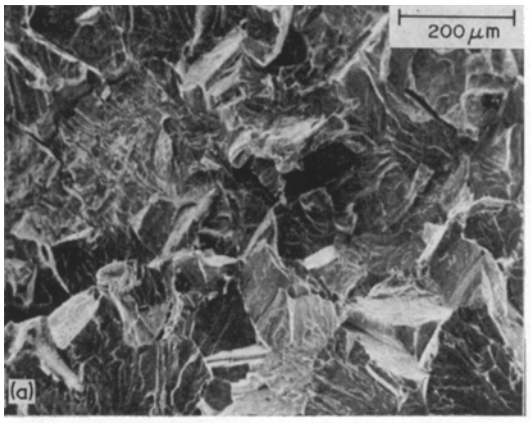

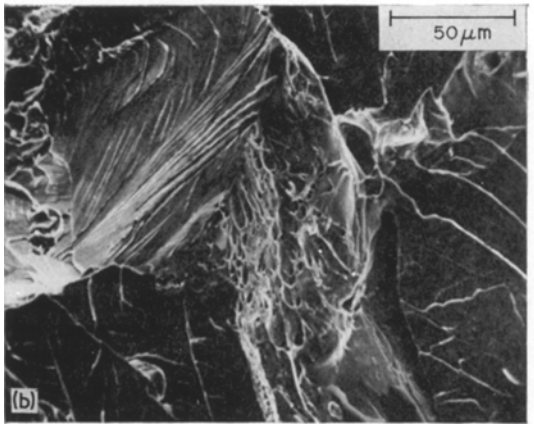

Figure 8 (a) Scanning electron micrograph of the fracture surface in an embrittled 21.8 at. % Al alloy showing predominant transgranular fracture. Electron beam was oriented 43° with respect to the fracture surface. (b) Higher magnification scanning electron micrograph from a different area of the same sample from which (a) was obtained, showing both river patterns along with void formation.

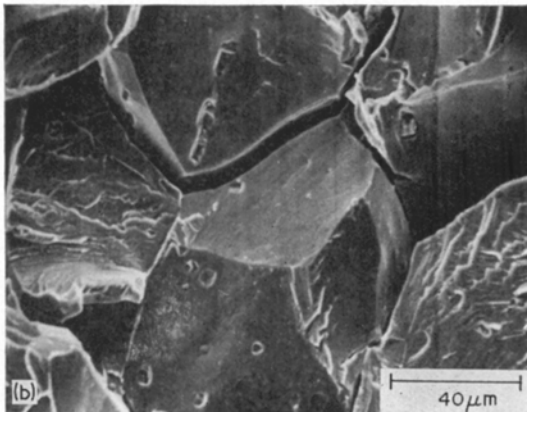

Figure 9 (a) Scanning electron micrograph of the fracture surface in a fully embrittled 25.5 at. % Al alloy exhibiting intergranular fracture. Electron beam was oriented 43° with respect to the fracture surface. (b) High magnification scanning electron micrograph of the central area shown in (a).

with the Fe–Al phase diagram shows that the rapid decrease in ductility which occurs at about 20 at. % Al closely parallels the onset of long range order at this composition [12]*. The somewhat slower decrease in ductility with Al content for concentrations less than 20 at. % Al may be associated with increasing amounts of short range atomic order. It is well known that long range atomic order [36], and to a lesser extent short range atomic order [37], favour the formation of superlattice dislocations, i.e. ordinary dislocations which bound ribbons of antiphase boundaries (APBs).

Such dislocations can move through the crystal with relative ease, compared to the corresponding ordinary dislocations which leave in their wake ribbons of disorder or APBs. On the other hand, cross-slip of superlattice dislocations is extremely difficult, since work must be done against the APB tension [38-40]. It has been shown that double cross-slip is a very effective means for obtaining slip multiplication, with the subsequent formation of pronounced slip bands [41]. The observation that long range

*One of us (FXK) used X-ray diffraction, electrical resistivity and precision density measurements to determine the long range order boundary for this specimen set. For temperatures near room temperature, the boundary occurred at 20.4 ± 0.1 at % Al.

atomic ordering favours the formation of very fine uniform slip lines rather than slip bands [42, 43] is further confirmation of the difficulty of cross-slip in ordered alloys.

The relationship between cross-slip and fracture surface morphology can be seen by first referring to Fig. 10. In particular, Fig. 10a shows a hole within a solid which is being subjected to a tensile stress σ. It has been shown [29, 44] that the state of stress associated with such a hole can be described in terms of an array of half dislocations which are designated as horizontal L's. These may be termed hole dislocations and are similar to crack dislocations into which the hole dislocations would degenerate if the vertical dimension of the hole were reduced to some small value approaching zero. The stress fields associated with the hole dislocations are sufficient to generate crystal lattice dislocation loops such as shown in Fig. 10b. A portion of the loop is attracted to the hole, while the remaining part of the loop, which is of opposite sign, moves into the interior of the crystal, away from the hole. In this way, the hole is enlarged. In order for the hole to enlarge uniformly, as is in fact observed to be the case in the more ductile low Al content Fe–Al alloys, profuse crystal lattice dislocation generation on numerous slip planes must occur in the vicinity of the hole. Such profuse slip generation is most readily provided by the double cross-slip mechanism of Koehler [41]. In the case of the long range ordered Fe–Al alloys, and to a smaller extent in the short range ordered alloys, the difficulty in cross-slip either limits or eliminates completely the nucleation and growth of voids, in accordance with the present observations.

Since the absence of void formation appears to be synonymous with brittle fracture in the present alloys, two alternatives present themselves: transgranular and intergranular fracture as observed in Figs. 7 and 8 respectively. It has already been argued in connection with the simple ordered structure of Fig. 1 that intergranular fracture should be favoured in ordered alloys because of the disorder associated with the grain boundaries. This reasoning also holds for the specific case of the Fe_3Al alloy, as can be seen in Fig. 11. In particular, within each grain interior, the ordered configuration of atoms is such that Al atoms form neither first nor second nearest neighbours with one another. However, incorrect Al atom neighbours are seen to exist across the 53.1° symmetric tilt boundary

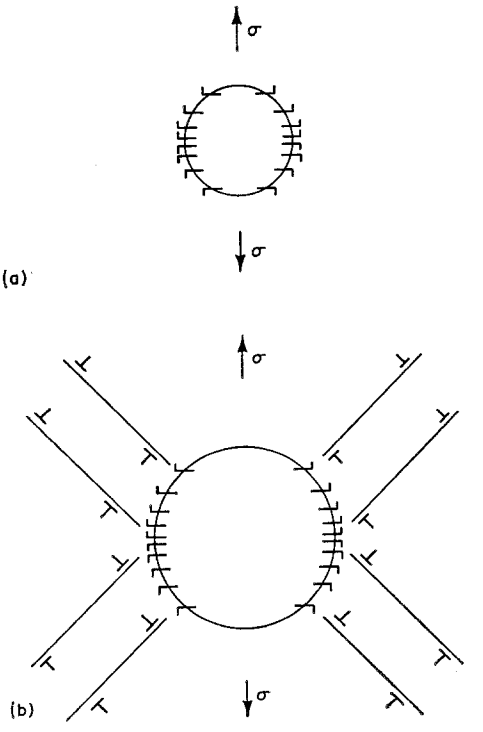

Figure 10 (a) Hole dislocations within a stressed hole. (b) Enlargement of stressed hole in (a) by the generation of crystal lattice dislocations.

shown in Fig. 11. A more detailed description of grain boundaries in body centred cubic structures can be obtained in [45] and [46]. The above postulates are in agreement with the observations of intergranular fracture observed in those alloys containing approximately 25 at. % or more Al as can be seen in Fig. 8. On the other hand, in order to explain the transgranular fractures observed in those long range ordered alloys containing less than 25 at. % Al, reference is made to the schematic illustration shown in Fig. 12. An ordinary dislocation is seen to emanate from the grain boundary with the consequent production of an APB (shown shaded). Such generation of ordinary dislocations has been shown to occur quite commonly in the lower Al content long range ordered Fe–Al alloys [10, 12]. As in the case of high-angle boundaries, these APBs are also of relatively high energy and can thus provide an alternate path for crack propagation through the grain interiors. Alternately, when a low-angle boundary terminates on a high-angle boundary, as illustrated in Fig. 12, the low-angle boundary may also provide an alternate high energy for a

propagating crack since, as noted earlier, such low-angle boundaries also possess large amounts of disorder. Extensive transmission electron microscopy observations with FeCo has, in fact, shown large numbers of low-angle boundaries attached to high-angle boundaries [46]. It has been argued that such low-angle boundaries may be relatively more stable in the less stoichiometric superlattices since less disorder is associated with such boundaries [47]. The transgranular fracture modes observed in Fig. 7 for the 21.8 at. % Al alloy can thus be accounted for on the basis of the above arguments.

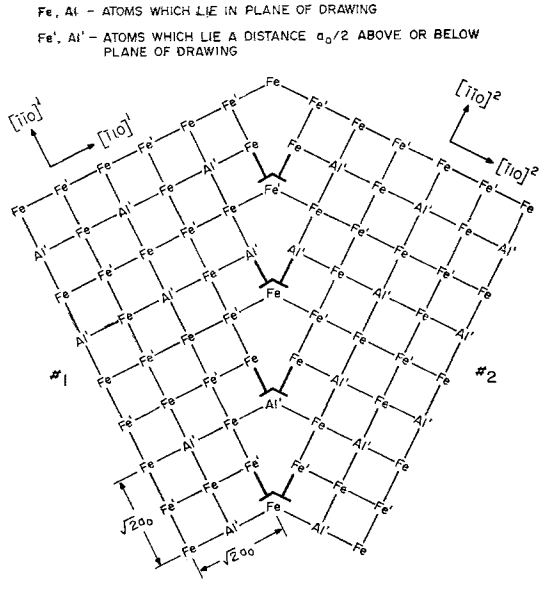

Figure 11 Symmetrical high-angle tilt boundary with a coincidence angle of 53.1° in an ordered Fe_3Al alloy. Rotation axis is along [001] and is normal to the drawing.

Some further insight in the brittle fracture associated with the long range ordered Fe–Al alloys can also be obtained by considering a theory first proposed by Cottrell [48] which can be written in the form of the following relation

$$\sigma_y k_y d^{1/2} \geqslant \beta\mu\gamma$$

where σ_y is the yield stress of the alloy, k_y is the Hall-Petch slope, d is the grain diameter, β is a constant in the order of 1, μ is the shear modulus, and γ is the surface energy associated with crack formation. Any change that increases the left side of the above equation with respect to the right side will favour brittle fracture. It is well known that atomic ordering significantly increases k_y [47, 49], and as the previous arguments have shown, γ is lowest along both high- and low-angle boundaries, as well as APBs, when compared to fracture paths within the more perfectly ordered grain interiors.

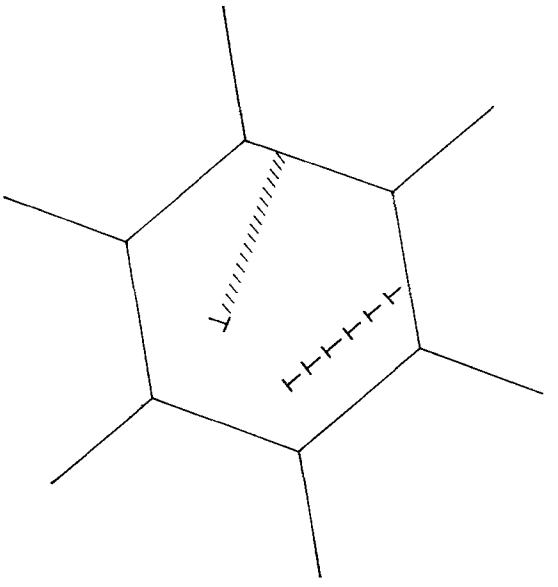

Figure 12 Slip produced antiphase boundary and low-angle boundary, both of which are attached to high-angle boundaries, and which could provide alternate high energy paths for crack propagation.

4. Summary and conclusions

A scanning electron microscopy study has been carried out of the fracture surfaces obtained from slowly cooled Fe–Al alloys pulled in tension and containing up to 28 at. % Al. It has been found that alloys possessing up to about 20 at. % Al fractured in a ductile manner by void nucleation and coalescence. However, alloys containing up to about 25 at. % Al failed in a brittle manner by a transgranular mode, while those possessing higher Al concentrations fractured intergranularly in a brittle manner. The loss of ductility and resulting brittle fracture is associated with the retardation of cross-slip occasioned by the onset of long range atomic order. On the other hand, the change in brittle fracture from transgranular to intergranular is related to the decrease in slip produced APBs and/or low-angle boundaries within the grain interiors. The high-angle grain boundaries, with their relatively large degree of disorder, thus provide the only high energy paths along which crack propagation

can occur. In no case was it found necessary to associate the fracture behaviour of the present alloys with impurity segregation at the grain boundaries.

Acknowledgements

The authors would like to express their thanks to Professor R. W. Armstrong of the Engineering Materials Group of the University of Maryland, for several very helpful discussions during the course of this investigation. In addition, they would also like to acknowledge the use of the Electron Microscope Central Facility of the Center of Materials Research at the University of Maryland, in which all of the present scanning electron microscopy studies were carried out. Finally, support for the present research was made available through a grant from the United States Atomic Energy Commission under Contract Number AT-(40-1)-3935.

References

1. M. J. MARCINKOWSKI and JAMES LARSEN, *Met. Trans.* **1** (1970) 1034.
2. SHENG-TI FONG, M. J. MARCINKOWSKI and K. SADANANDA, *Acta Metallurgica* **21** (1973) 799.
3. M. J. MARCINKOWSKI and D. S. MILLER, *Phil. Mag.* **6** (1961) 871.
4. P. F. TIMMINS and A. S. WRONSKI, *Nature, Phys. Sci.* **235** (1972) 113.
5. N. S. STOLOFF and R. G. DAVIES, *Acta Metallurgica* **12** (1964) 473.
6. T. L. JOHNSTON, R. G. DAVIES and N. S. STOLOFF, *Phil. Mag.* **12** (1965) 305.
7. J. F. DINHUT, J. P. EYMERY and P. MOINE, *Phys. Stat. Sol.* **12a** (1972) 153.
8. K. R. JORDAN and N. S. STOLOFF, *Trans. Met. Soc. AIME* **245** (1969) 2027.
9. *Idem, Jap. Inst. Metals, Suppl.* **9** (1968) 281.
10. H. J. LEAMY and F. X. KAYSER, *Phys. Stat. Sol.* **34** (1969) 765.
11. F. X. KAYSER, Ford Motor Co., WADC Tech. Report 57-298 Part I (1957).
12. H. J. LEAMY, Ph.D. Thesis, Iowa State University (1967).
13. GORDON E. LAKSO, M.S. Thesis, Iowa State University (1966).
14. A. R. BAILEY, R. MCDONALD and L. E. SAMUELS, *J. Inst. Metals* **85** (1956-57) 25.
15. S. HARPER, *J. Metals* **85** (1956-57) 415.
16. A. A. PRESNYAKOV and G. V. STARIKOVA, *Phys. Met. Metallogr.* **12** (6) (1961) 84. Original: *Fiz. Metal. Metalloved.* **12** (1961) 873.
17. A. BALL and R. E. SMALLMAN, *Acta Metallurgica* **14** (1966) 1349.
18. E. M. GRALA, "Mechanical Properties of Intermetallic Compounds" edited by J. H. Westbrook, (Wiley, New York, 1960) p. 358.
19. N. S. STOLOFF and I. L. DILLAMORE, "Ordered Alloys – Structural Applications and Physical Metallurgy" edited by B. H. Kear, C. T. Sims, N. S, Stoloff and J. H. Westbrook (Claitor's, Baton Rouge. 1970) p. 525.
20. R. C. BOETTNER, N. S. STOLOFF and R. B. DAVIES, *Trans. Met. Soc. AIME* **236** (1966) 131.
21. H. D. WILLIAMS and G. C. SMITH, *Phil. Mag.* **13** (1966) 835.
22. J. H. WESTBROOK, *Met. Rev.* **9** (1965) 415.
23. A. V. SEYBOLT and J. H. WESTBROOK, *Acta Metallurgica* **12** (1964) 449.
24. M. J. MARCINKOWSKI, *Phil. Mag.* **17** (1968) 159.
25. J. CZERNICHOW, J. P. GUDAS, M. J. MARCINKOWSKI and WEN FENG TSENG, *Met. Trans.* **2** (1971) 2185.
26. M. J. MARCINKOWSKI, K. SADANANDA and WEN FENG TSENG, *Phys. Stat. Sol.* **17a** (1973) 423.
27. M. J. MARCINKOWSKI, E. S. P. DAS and K. SADANANDA, *ibid* **19a** (1973) 67.
28. M. J. MARCINKOWSKI, *Mém. Sci. Rev. Met.* **69** (1972) 579.
29. *Idem*, "Electron Microscopy and Structure of Materials", edited by G. Thomas, R. M. Fulrath and R. M. Fisher (University of California Press, Berkeley, 1972) p. 382.
30. F. X. KAYSER, *J. Metals* **10** (1958) 573.
31. F. X. KAYSER and E. O. MARANDE, to be published.
32. C. D. BEACHEM, "Fracture", Vol. 1, edited by Harold Liebowitz (Academic Press, New York, 1968) p. 243.
33. V. F. ZACKAY, W. W. GERBERICH and E. R. PARKER, *ibid* p. 395.
34. J. FRIEDEL, "Dislocations" (Addison-Wesley, Reading, Mass., 1964).
35. J. R. LOW, "Deformation and Flow of Solids" edited by R. Grammel (Springer-Verlag, Berlin, 1956) p. 60.
36. M. J. MARCINKOWSKI, "Electron Microscopy and Strength of Solids" edited by G. Thomas and J. Washburn (Interscience, New York, 1963) p. 333.
37. W. BELL, W. R. ROSEN and G. THOMAS, *Acta Metallurgica* **12** (1964) 1247.
38. M. J. MARCINKOWSKI and HENRY CHESSIN, *Phil. Mag.* **10** (1964) 837.
39. N. S. STOLOFF and R. G. DAVIES, *Acta Metallurgica* **12** (1964) 473.
40. M. J. MARCINKOWSKI, N. J. OLSON and K. SADANANDA, *Phys. Stat. Sol.* **17a** (1973) 89.
41. J. S. KOEHLER, *Phys. Rev.* **86** (1952) 52.
42. T. TAOKA and S. SAKATA, *Acta Metallurgica* **5** (1957) 61.
43. T. TAOKA and R. HONDA, *J. Electron Microscopy* **5** (1957) 19.
44. M. J. MARCINKOWSKI and E. S. P. DAS, *Int. J. Fracture* **10** (1974) 181.
45. M. J. MARCINKOWSKI, WEN FENG TSENG and E. S. DWARAKADASA, *J. Mater. Sci.* **9** (1974) 29.

46. WEN FENG TSENG, M. J. MARCINKOWSKI and E. S. DWARAKADASA, *ibid* **9** (1974) 41.

47. M. J. MARCINKOWSKI, "Treatise on Materials Science and Technology", Vol. 5, edited by H. Herman, (Academic Press, New York, 1974) p. 181.

48. A. H. COTTRELL, *Trans. Met. Soc. AIME* **212** (1958) 192.

49. M. J. MARCINKOWSKI and R. M. FISHER, *Trans. Met. Soc. AIME* **233** (1965) 293.

Received 22 July and accepted 28 August 1974.